CENTER FOR INFRASTRUCTURE ENGINEERING STUDIES

Determination of SASW Shear-Wave Velocity Along a Segment of Interstate 70 in St. Louis, Missouri

By

Dr. Neil Anderson

T. Thitimakorn

UTC R100

University Transportation Center Program at

The Universitv of Missouri-Rolla

Disclaimer

The contents of this report reflect the views of the author(s), who are responsible for the facts and the accuracy of information presented herein. This document is disseminated under the sponsorship of the Department of Transportation, University Transportation Centers Program and the Center for Infrastructure Engineering Studies UTC program at the University of Missouri - Rolla, in the interest of information exchange. The U.S. Government and Center for Infrastructure Engineering Studies assumes no liability for the contents or use thereof.

Technical Report Documentation Page

1. Report No.	2. Government Accession No.	3. Recipient's Catalog No.
UTC R100		

4. Title and Subtitle	5. Report Date
Determination of SASW Shear-Wave Velocity Along a Segment of Interstate 70 in St. Louis, Missouri	Dec 2004
	6. Performing Organization Code

7. Author/s	8. Performing Organization Report No.
Dr. Neil Anderson, T. Thitimakorn	00000825

9. Performing Organization Name and Address	10. Work Unit No. (TRAIS)
Center for Infrastructure Engineering Studies/UTC program University of Missouri - Rolla 223 Engineering Research Lab Rolla, MO 65409	11. Contract or Grant No. DTRS98-G-0021

12. Sponsoring Organization Name and Address	13. Type of Report and Period Covered
U.S. Department of Transportation Research and Special Programs Administration 400 7th Street, SW Washington, DC 20590-0001	Final
	14. Sponsoring Agency Code

15. Supplementary Notes

16. Abstract

The University of Missouri-Rolla (UMR) proposes to acquire multi-channel surface-wave (seismic analysis of surface waves; SASW) seismic data along a test segment (~8000 lineal foot transect) of interstate I-70 in downtown St. Louis. These SASW data will be processed and analyzed (seismic analysis of surface waves), and used to construct subsurface shear-wave velocity profiles (to depths on the order of 50 feet) at station intervals on the order of 40 feet. The main project deliverable will be a cross-sectional transect (along the test segment of interstate) depicting estimated depth to bedrock and spatial variations in the shear-wave velocity of the soil and bedrock.

17. Key Words	18. Distribution Statement
Non-destructive imaging, non-invasive imaging, technology transfer, education.	No restrictions. This document is available to the public through the National Technical Information Service, Springfield, Virginia 22161.

19. Security Classification (of this report)	20. Security Classification (of this page)	21. No. Of Pages	22. Price
unclassified	unclassified		

Form DOT F 1700.7 (8-72)

EXECUTIVE SUMMARY

The University of Missouri-Rolla (UMR) acquired multi-channel surface-wave (Rayleigh wave) seismic control along a 6400 ft segment of interstate I-70, in downtown St. Louis, Missouri. The acquired surface wave data set was processed (multi-channel analysis of surface waves; MASW) and transformed into a 2-D MASW shear-wave velocity profile with a lateral station-spacing of 40 ft. The 2-D MASW profile extends from the surface to a depth of 50 ft. The interpreted depth to acoustic bedrock along the length of the 2-D profile varies between 20 ft and 44 ft.

The interpreted 2-D MASW shear-wave velocity profile was compared to available bedrock (borehole) and seismic cone penetrometer (SCPT) control provided by the Missouri Department of Transportation (MoDOT). The geotechnical data provided by MoDOT and presented herein indicate the interpreted 2-D MASW shear-wave velocity profile correlates well with available bedrock and SCPT control, supporting the conclusion that the MASW technique can be used to generate reliable 2-D shear-wave velocity profiles of the shallow subsurface.

ACKNOWLEDGEMENTS

The principal investigators would like to thank Mr. Tom Fennessey, PE, Missouri Department of Transportation, for his support, encouragement and direction.

TABLE OF CONTENTS

LIST OF FIGURES

LIST OF TABLES

1. INTRODUCTION

In May 2003, the University of Missouri-Rolla (UMR) acquired multi-channel surface-wave (Rayleigh wave) seismic control along a 6400 ft segment of interstate I-70, in downtown St. Louis, Missouri (MASW stations #1 to #161; Figures 1a-1d). The acquired surface wave data were processed (multi-channel analysis of surface waves; MASW) and transformed into a 2-D MASW shear-wave velocity profile consisting of more than 160 separate traces (vertical shear-wave velocity curves) spaced at 40 ft station intervals. The initial output MASW shear-wave velocity profile extended to a depth in excess of 100 ft. The 2-D MASW profile presented herein however, was truncated at a depth of 50 ft. This depth is sufficient to image the interpreted top of bedrock ($\leq$44 ft) and provides for superior visual resolution.

Herein, non-interpreted and interpreted versions of the 2-D MASW shear-wave velocity profile are presented. The interpreted 2-D MASW profile is compared to proximal bedrock (borehole) and seismic cone penetrometer (SCPT) control provided by the Missouri Department of Transportation (MoDOT). This comparative analysis supports two conclusions. First, the MASW technique can be used to generate reliable subsurface shear-wave velocities. Second, the top of acoustic bedrock can be identified and mapped with confidence on the MASW shear-wave velocity profile.

This MASW project is consistent with MoDOT's Research Focus Plan wherein the evaluation of recently-developed surface (Rayleigh) wave technology was identified as a priority for the Geotechnical Research and Development Technology Technical Advisory Group (RDT TAG) during the MOTREC/MoDOT biennial meeting (8/7/01). (MOTREC: Missouri Transportation Research Education Center.)

2. STATEMENT OF PROBLEM/SCOPE OF WORK

MoDOT was interested in evaluating the utility of the MASW technique. More specifically, MoDOT wanted to determine if the subsurface shear-wave velocity functions generated by the non-invasive MASW technique were reliable. MoDOT also wanted to determine if the MASW tool could be used to create reliable and interpretable 2-D shear-wave velocity profiles. If the MASW technique proved to be reliable and cost-effective, it could represent an alternative to the seismic cone penetrometer tool.

The determination or estimation of the in-situ shear modulus of shallow unconsolidated soil and bedrock is critically important in terms of the evaluation of foundation integrity. This is particularly true in terms of assessing the soil's response to strong ground motion.

Historically, MoDOT engineers have estimated the shear modulus of soils on the basis of standard penetration tests (SPT) and laboratory strain tests. More recently, MoDOT has estimated shear modulus on the basis of seismic cone penetrometer tests (SCPT). As noted in the following text, the SCPT tool has its own characteristic strengths and weaknesses.

Overview of Seismic Cone Penetrometer Test (SCPT) Technique: As utilized by MoDOT, this technique employs a downhole shear-wave geophone (acoustic receiver coupled to the tip of the SCPT cone) and a surface hammer shear-wave source. As the SCPT cone is pressed into the soil, it is halted momentarily at predetermined incremental depths (the center-to-center spacing of these "unit layers" is generally on the order of 1 m) and the surface shear-wave source is discharged twice – with opposite directional impacts - thereby generating two opposite-polarity shear-wave records.

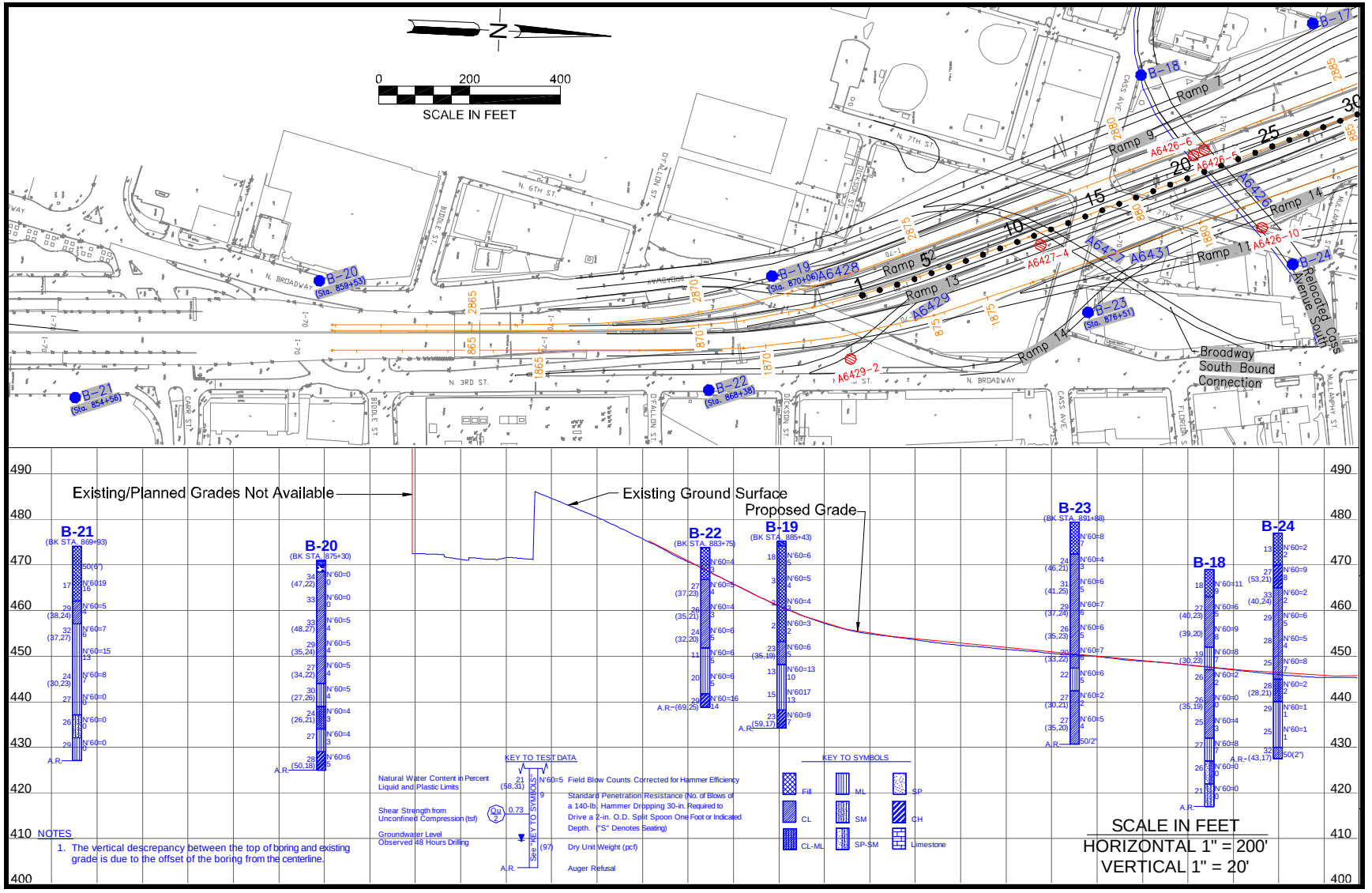

Figure 1a: Base map showing locations of MASW stations 1-30.

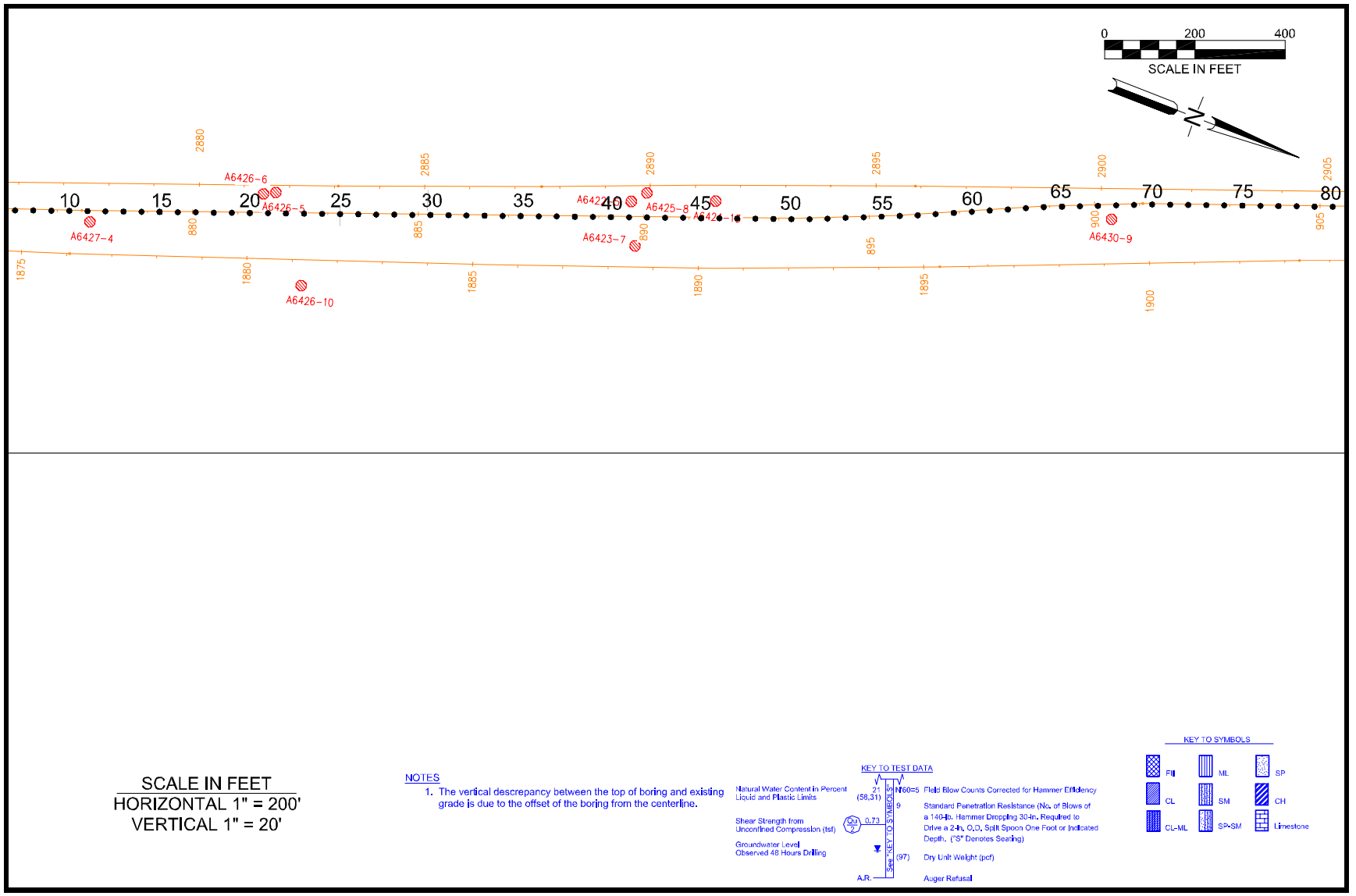

Figure 1b: Base map showing locations of MASW stations 7-80.

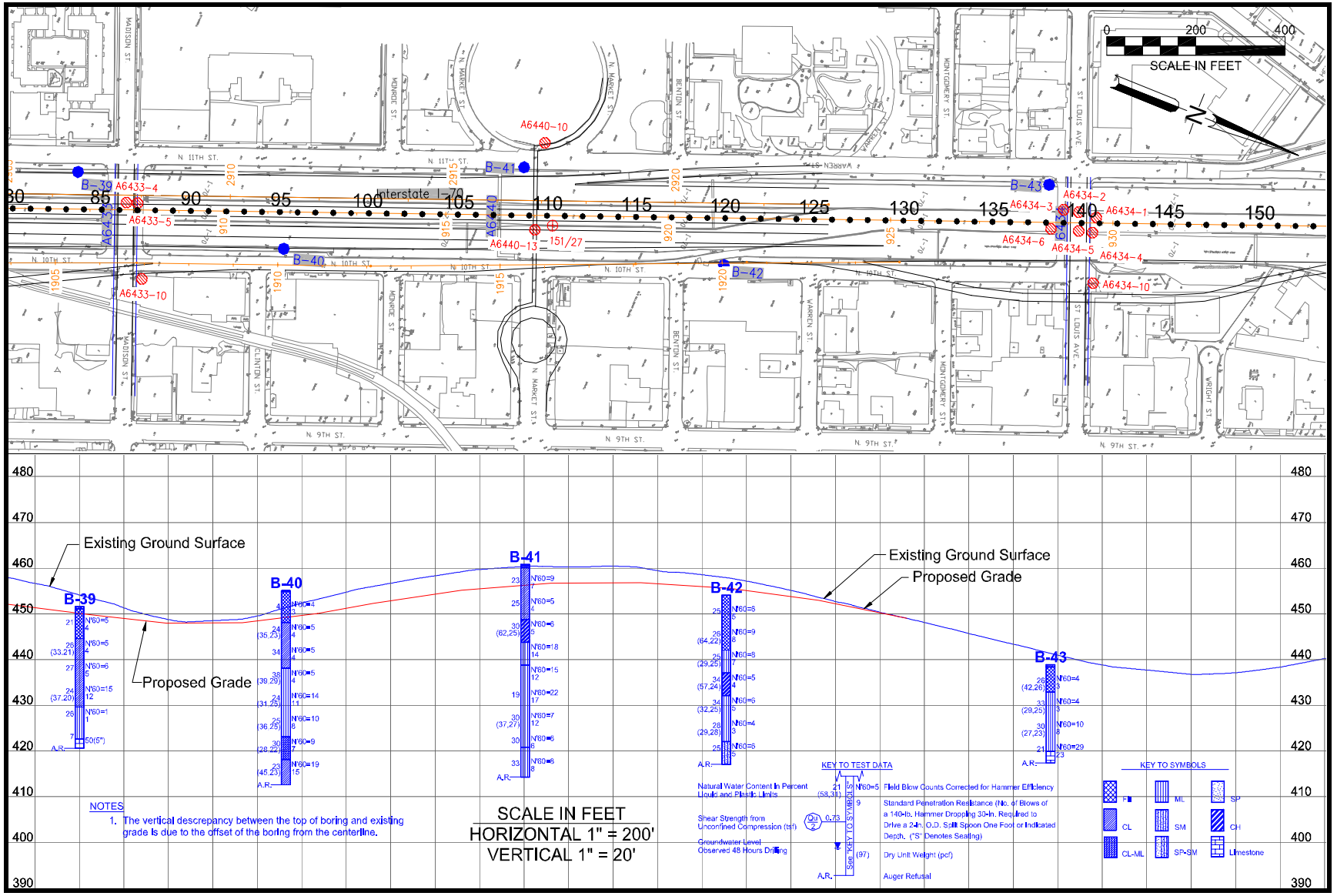

Figure 1c: Base map showing locations of MASW stations 80-153.

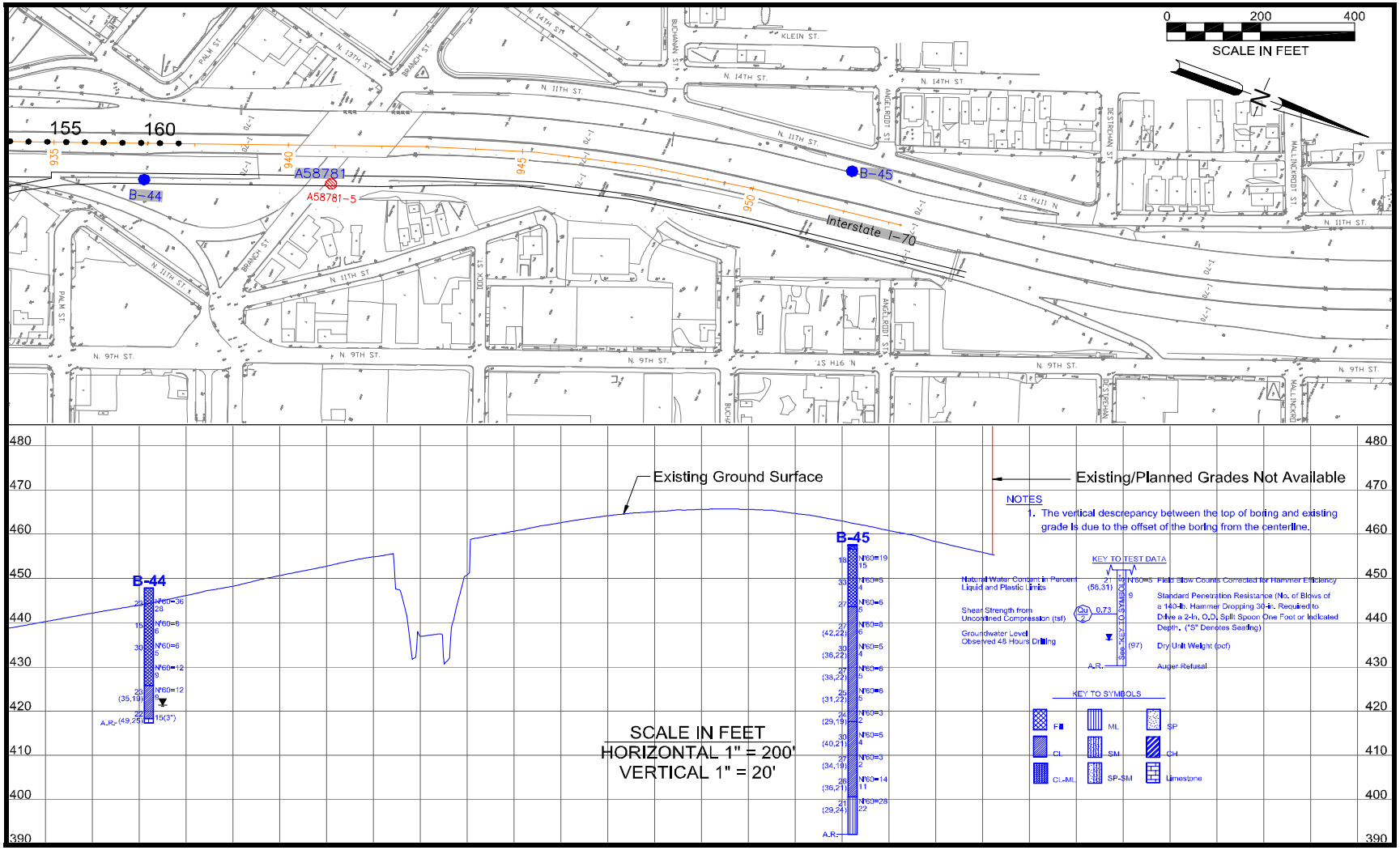

Figure 1d: Base map showing locations of MASW stations 152-161.

The arrival time of the shear-wave energy (travel time from source to geophone) is measured at the top of each layer ($\mathbf{Tn_{top}}$) and at the base of each layer ($\mathbf{Tn_{base}}$). The average shear-wave interval velocity ($\mathbf{\beta n_{int}}$) for the nth layer is then calculated as:

$$\mathbf{\beta n_{int} = \Delta Zn/\Delta Tn} \qquad \text{Equation 1}$$

where:

$\mathbf{\beta n_{int}}$ = shear wave interval velocity for nth layer
$\mathbf{\Delta Zn}$ = "acoustic" thickness of nth layer = $\mathbf{Ln_{top} - Ln_{base}}$
$\mathbf{Ln_{top}}$ = source-to-geophone separation at top of nth layer
$\mathbf{Ln_{base}}$ = source-to-geophone separation at base of nth layer
$\mathbf{\Delta Tn}$ = transit time through nth layer = $\mathbf{Tn_{top} - Tn_{base}}$
$\mathbf{Tn_{top}}$ = travel time from hammer source to geophone at top of nth layer
$\mathbf{Tn_{base}}$ = travel time from hammer source to geophone at base of nth layer

If the arrival times ($\mathbf{Tn_{top}}$; $\mathbf{Tn_{base}}$) of the shear wave energy at the top and base each layer are accurately determined and if the source-to-geophone separations are accurately measured, the SCPT tool is capable of providing accurate subsurface shear-wave interval velocities ($\mathbf{\beta n_{int}}$). However, if arrival times are not accurately determined, the output shear-wave interval velocities will be inaccurate. There are two most-probable causes of such error. First, it is conceivable that earlier arriving compressional-wave (P-wave) energy (upgoing and/or downgoing) could be misinterpreted as shear-wave energy, particularly at shallow receiver depths (where the P-wave and S-wave arrivals are almost superposed). A second possible cause of "error" is related to the accuracy with which shear-wave arrival times can be determined at each test depth. Even in those situations where shear-wave energy is clearly differentiated from earlier arriving compressional wave energy, there is some intrinsic uncertainty in the determination of shear-wave arrival times. Small errors (e.g. $\pm$1 ms) in estimated transit time ($\mathbf{\Delta Tn}$) through the nth layer will generate corresponding errors in the estimated shear-wave interval velocities ($\mathbf{\beta n_{int}}$) assigned to the nth layer. For example, if the transit time ($\mathbf{\Delta Tn}$) through a 1 m thick layer (with a shear-wave velocity of 250 m/s) is underestimated by 1 ms, the interval velocity ($\mathbf{\beta n_{int}}$) assigned to that layer will be overestimated by 33%.

If the interval shear-wave velocity ($\mathbf{\beta n_{int}}$) assigned to the nth layer is inaccurate (i.e., too high or too low, as discussed above), the shear-wave interval velocity ($\mathbf{\beta n+1_{int}}$) assigned to the underlying layer (n+1th) layer will also be inaccurate (i.e., too low or too high, respectively; assuming of course that arrival times of shear-wave energy is correctly determined for n+1th layer).

Inaccurate determinations of the source-to-geophone separations ($\mathbf{Ln_{top}}$, $\mathbf{Ln_{base}}$) will similarly result in inaccurate shear-wave interval velocity estimates ($\mathbf{\beta n_{int}}$).

In terms of overall utility, the SCPT tool works well in clays, silts and sands – but doesn't work well in gravels (which can damage the cone head). Also, the SCPT tool can access only those sites accessible to conventional tracked equipment.

Summary: As noted in the preceding text, the SCPT tool has characteristic strengths and weaknesses. In an attempt to evaluate an alternate, recently-developed methodology that could prove to be more effective than conventional techniques at certain sites, MoDOT asked UMR researchers to acquire surface wave (Rayleigh wave) seismic data along a 6400 ft segment of interstate I-70 in downtown St. Louis, Missouri (Figures 1a-1d). These surface-wave data were processed (inverted) and transformed into a 2-D MASW shear-wave velocity profile. This 2-D MASW profile consists of more than 160 separate stations (vertical shear-wave velocity curves) spaced at 40 ft intervals.

3. OBJECTIVE

The objective of this study was to acquire MASW (Rayleigh wave) data along a 6400 ft segment of interstate I-70 in downtown St. Louis (Figures 1a-1d). The intent was to process (through spectral inversion) these Rayleigh wave data and generate a 2-D MASW shear-wave velocity profile consisting of multiple stations (shear-wave velocity curves) spaced at 40 ft station intervals. This 2-D MASW profile was to be interpreted and compared with proximal borehole control (provided by MoDOT).

There were two primary goals. The first was to determine if the shear-wave velocity functions generated by the non-invasive MASW technique were reliable. The second was to determine if the MASW tool could be used to create a reliable and interpretable 2-D shear-wave velocity profile. If the MASW technique proved to be reliable and cost-effective – it could represent an alternative to conventional methodologies, including the SCPT technique.

4. A BRIEF OVERVIEW OF INDUCED SEISMIC WAVES

When an acoustic source (weight drop, dynamite charge, etc.) is discharged at or near the surface of the earth, two fundamental types of acoustic waves (strain energy) are produced: body waves and surface waves. Two types of body waves can propagate through an elastic solid (compressional waves and shear waves). Similarly, two types of surface waves can propagate along the earth's surface (Rayleigh waves and Love waves).

Compressional waves (or P-waves) propagate by compressional and dilatational strains in the direction of wave travel (Figure 2). Particle motion involves oscillation, about a fixed point, in the direction of wave propagation. Shear waves (or S-waves) propagate by a pure strain in a direction perpendicular to the direction of wave travel (Figure 2). Body waves are essentially non-dispersive over the range of frequencies employed for earthquake studies and seismic exploration (i.e., all component frequencies propagate at the same velocity). The propagation velocities of body waves are a function of the engineering properties of the medium through which they are traveling (Figure 2).

Love waves propagate along the surface of a layered solid (earth's surface) if the shear-wave velocity of the uppermost layer is lower than that of the underlying layer (e.g., unconsolidated strata overlying bedrock). Love waves are polarized shear waves with an oscillatory particle motion parallel to the free surface and perpendicular to the direction of wave motion (Figure 3). Love waves are dispersive, and are characterized by velocities between the shear-wave velocity of the shallowest layer and that of deeper layers. The amplitude of a Love wave decreases exponentially with depth. The lower component frequencies of Love waves involve particle motion at greater depth and therefore generally exhibit higher velocities.

Rayleigh waves propagate along the earth's surface (free surface). The associated particle motion is elliptical in a plane perpendicular to the surface and containing the direction of propagation (Figure 3). The orbital motion is in the opposite sense to the circular motion associated with a water wave, and is often described as retrograde elliptical. The amplitude of a Rayleigh wave decreases exponentially with depth (Figure 3). Progressively lower frequency components of Rayleigh waves involve particle motion over progressively greater depth ranges (relative to free surface). Rayleigh waves in a heterogeneous medium (with respect to velocity) are therefore dispersive. The velocities with which the highest component frequencies travel are a function of the engineering properties of the shallowest sediment. The velocities with which progressively lower frequencies travel are functions of the varying engineering properties over a progressively greater range of sediment depths. In the "multi-channel analysis of surface wave" (MASW) technique, the phase velocities of the component frequencies are calculated. These data are then inverted and used to generate a vertical shear-wave velocity profile.

5. RAYLEIGH WAVES (OVERVIEW OF MASW TECHNIQUE)

Rayleigh waves propagate along the free surface of the earth, with particle motions that decay exponentially with depth (Figure 3). The lower component frequencies of Rayleigh waves involve particle motion at greater depths. In a homogeneous (non-dispersive) medium, Rayleigh wave phase velocities are constant can be determined using the following equation:

$$V_R^6 - 8\beta^2 V_R^4 + (24 - 16\beta^2/\alpha^2)\beta^4 V_R^2 + 16(\beta^2/\alpha^2 - 1)\beta^6 = 0 \qquad \text{Equation 2}$$

where:

V_R is the Rayleigh wave velocity within the uniform medium
β is the shear-wave velocity within the uniform medium (also denoted Vs)
α is the compressional wave velocity within the uniform medium (also denoted Vp)

Rayleigh wave velocities, as noted in Equation 2, are a function of both the shear-wave velocity and compressional wave velocity of the subsurface.

In a heterogeneous earth, shear-wave and compressional-wave velocities vary with depth. Hence, the different component frequencies of Rayleigh waves (involving particle motion over different depth ranges) exhibit different phase velocities (Bullen, 1963). The phase velocity of each component frequency being a function of the variable body wave velocities over the vertical depth range associated with that specific wavelength. More specifically, in a layered earth, the Rayleigh wave phase velocity equation has the following form:

$$V_R(f_j, C_{Rj}, \beta, \alpha, \rho, h) = 0 \quad (j = 1, 2, \ldots, m) \qquad \text{Equation 3}$$

where:

f_j is the frequency in Hz
V_{Rj} is the Rayleigh-wave phase velocity at frequency f_j
$\beta = (\beta_1, \beta_2, \ldots, \beta_n)^T$ is the s-wave velocity vector
β_i is the shear-wave velocity of the *i*th layer
$\alpha = (\alpha_1, \alpha_2, \ldots, \alpha_n)^T$ is the compressional p-wave velocity vector
α_i is the P-wave velocity of the *i*th layer
$\rho = (\rho_1, \rho_2, \ldots, \rho_n)^T$ is the density vector
ρ_i is the density of the *i*th layer
$h = (h_1, h_2, \ldots, h_{n-1})^T$ is the thickness vector
h_i the thickness of the *i*th layer
n is the number of layers within the earth model

The spectral analysis of surface waves (MASW) technique is based on the relationship between Rayleigh wave phase velocities and the depth-range of associated particle motion. More specifically, in this technique, phase velocities are calculated for each component frequency of field-recorded Rayleigh waves (active monitoring). The resultant dispersion curve (phase velocity vs. frequency) is then inverted using a least–squares approach and a vertical shear-wave velocity profile is generated (Miller *et al.*, 2000; Nazarian *et al.*, 1983; Stokoe *et al.*, 1994; Park *et. al.,* 2001; Xia *et al.*, 1999).

(a) P-waves

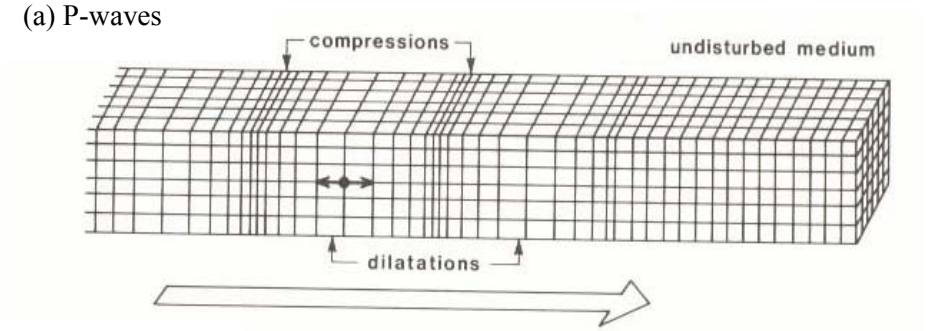

(b) S-waves

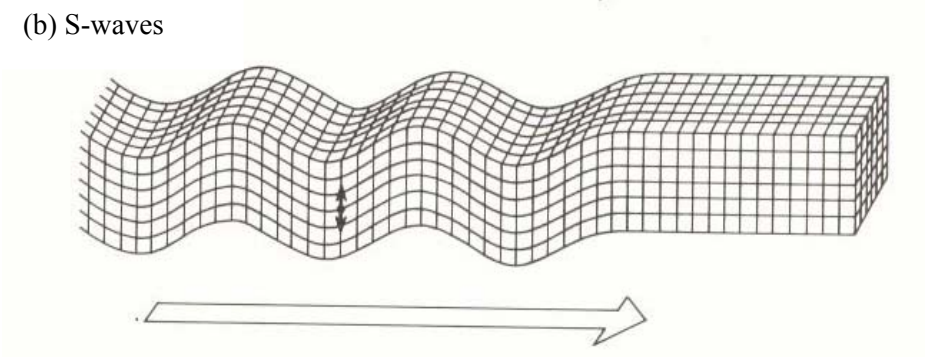

$\alpha = [(K + 4\mu/3)/\rho]^{1/2}$

$\beta = [\mu/\rho]^{1/2}$

where:

α = P-wave velocity (Vp)

β = S-wave velocity (Vs)

K = bulk modulus

μ = shear modulus

ρ = density

Figure 2: Particle motions associated with compressional waves (P-waves; upper caption) and shear waves (S-waves; lower caption).

(a) Rayleigh waves

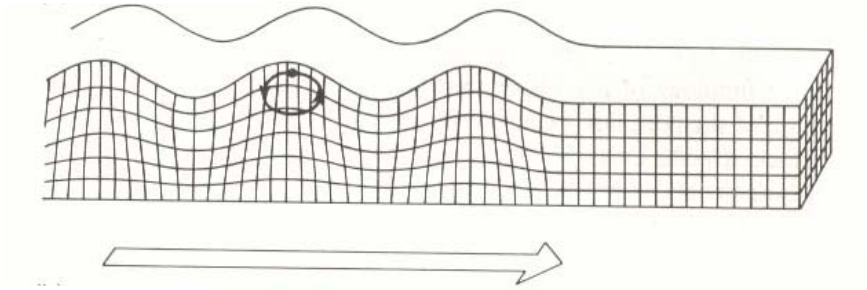

Rayleigh wave particle motion
- retrograde elliptical
- decreases exponentially with depth
- function of α and β

(b) Love waves

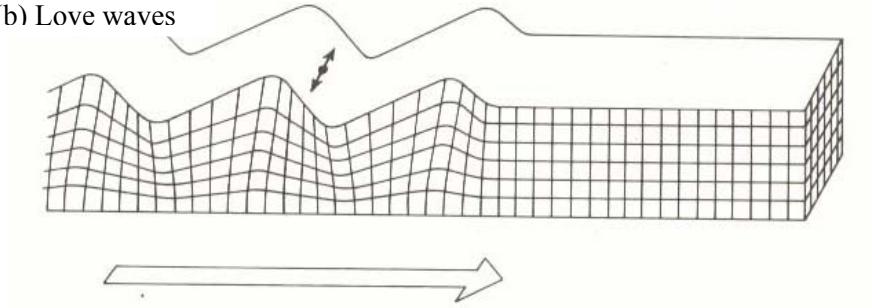

Love wave particle motion
- horizontal
- decreases exponentially with depth
- function of β

Figure 3: Particle motions associated with Rayleigh waves (upper caption) and Love waves (lower caption).

6. MASW FIELD TECHNIQUE

The acquisition of the "active" Rayleigh wave (surface wave) data was relatively straightforward (Figure 4). Essentially, 12 low-frequency (4.5 Hz) vertical geophones, placed at 10 ft intervals, were centered about station location #1 (Figures 1a-1d). Acoustic energy was generated at an offset (distance to nearest geophone) of 60 ft using a 20 lb sledge hammer and metal plate. The generated Rayleigh wave data were recorded. For "all intents and purposes", the entire 12-channel geophone array and source were then shifted (iteratively, and at 40 ft station intervals) along the entire test segment of interstate. At each "station" location, Rayleigh wave data were generated and recorded. (In actual fact, the MASW data were acquired using a 24-channel seismograph. Data acquisition was not quite as straightforward as described above, however it was much more efficient.)

7. PROCESSING OF MASW DATA

The acquired Rayleigh wave data were processed using the KGS software package SURFSEIS (Figure 5). Each set of Rayleigh wave data (12 channel data set for each station location) was transformed from the time domain into the frequency domain using Fast Fourier Transform (FFT) techniques. These field-based data were used to generate site-specific dispersion curves ($\mathbf{V_R(f)}$ versus $\boldsymbol{\lambda_R(f)}$) for each station location. The site-specific dispersion curves (**DCS**) generated from field-acquired Rayleigh wave data were then transformed into vertical shear-wave velocity profiles (**SASW** shear-wave velocity profile). Transformations were based on the assumption that Poisson's Ratio was 0.4. (Note: This ratio was recommended by Dr. Park, KGS, as a reasonable ratio for unsaturated, unconsolidated soil. According to Dr. Park and other references, Poisson's ratio for soils generally ranges from 0.38 - 0.48.)

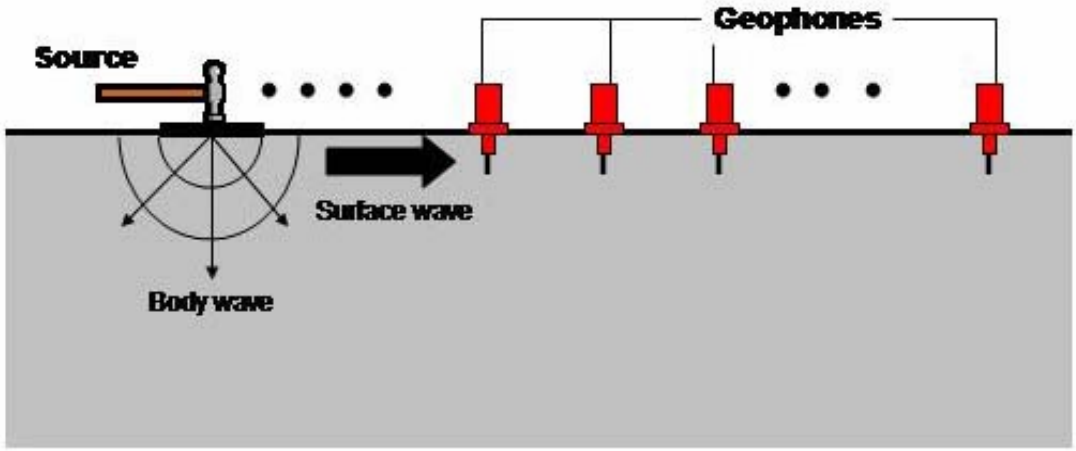

Figure 4: Field configuration. Each Rayleigh wave data set was recorded using an array consisting of 12 low-frequency geophones. The near shot-receiver offset was 60 ft.

8. MASW SHEAR-WAVE PROFILES: CONSIDERATIONS

Consideration A: Rayleigh-wave phase velocities were determined using a centered suite of 12 geophones spaced over a distance of 110 ft. The Rayleigh-wave phase velocities therefore represent "average" subsurface velocities determined over the breadth and depth of a 110 ft interval. Thus, the vertical shear-wave velocity profiles generated for each station location represent "average" subsurface velocities.

Consideration B: Rayleigh-wave data were acquired in a "noisy" environment (at times, vehicular traffic noise was intense). However, the background noise does not appear to adversely affect the overall reliability of the interpretations.

Consideration C: Transformations were based on the assumption that Poisson's ratio is 0.4. (Note: This ratio was recommended by Dr. Park, Kansas Geological Survey as a reasonable ratio for unsaturated, unconsolidated soil.) If this ratio is "overestimated", output shear-wave velocities and depth estimates (re: horizons) will be anomalously high. Conversely, if this ratio is "underestimated", output shear-wave velocities and depth estimates (re: acoustic bedrock) will be anomalously low.

Consideration D: Shear-wave velocities are determined sequentially (from shallowest interval to deepest interval). Thus any inaccuracies (with respect to the determination of shear-wave velocities at shallow depths) produce cascading errors. The result is that the accuracy of the shear-wave estimates tends to diminish with increasing depth.

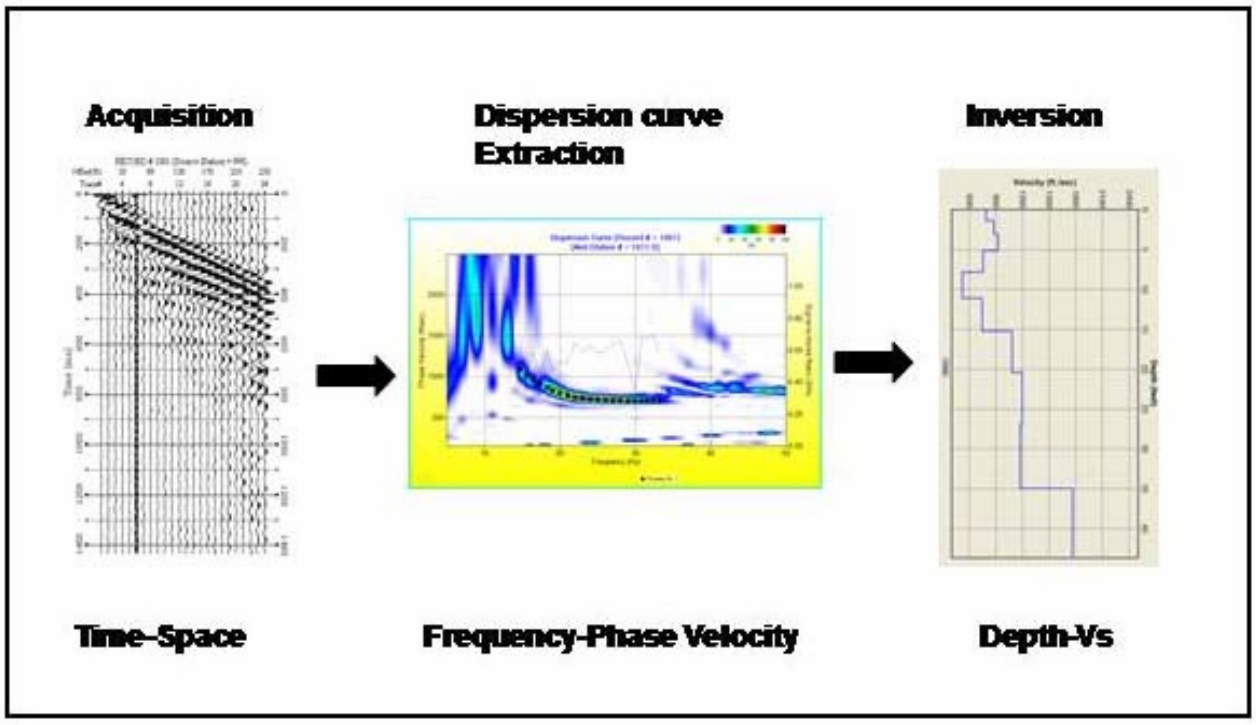

Figure 5: Dispersion curves were generated for each acquired Rayleigh wave data set. Each dispersion curve was transformed (inversion) into a shear-wave velocity vs. depth curve.

9. FIELD SITES: LOCATIONS AND GEOTECHNICAL DATA

The MASW data were acquired along a 6400 ft paved segment of interstate I-70 in downtown St. Louis (Figures 1a-1d). Borehole and SCPT control are depicted on these maps. Note, that all of the SCPT and most of the borehole sites are off-line (re: MASW profile). For the purposes of comparative analyses, borehole and SCPT data were "tied" to the closest MASW station location.

10. 2-D MASW SHEAR-WAVE VELOCITY PROFILE

The non-interpreted version of the MASW shear-wave velocity profile is presented as Figure 6. The interpreted version is presented as Figure 7. The "horizon" correlated (with minimal smoothing) across the MASW profile (depths of 20-44 ft; Figure 7) is interpreted as "acoustic bedrock". (Acoustic bedrock, as mapped on the MASW profile, is characterized by shear-wave velocities in excess of 1000 ft/s.) The identification of acoustic bedrock (Figure 7) was based on the "ties" between the 2-D MASW profile and the limited borehole control (boreholes B-39, B-43 and B-44) initially provided by MoDOT. At these three borehole locations and at all other test locations (except SCPT Site A6440-10), "acoustic" bedrock represents the soil/limestone interface. (At SCPT Site A6440-10, "acoustic" bedrock may correspond to the top of the dense sand immediately overlying bedrock.)

Limestone bedrock in the study area is characterized by MASW shear-wave velocities that typically increase from 1000 ft/s to in excess of 1500 ft/s over vertical depths on the order of 15 ft (Figure 7). This increase in velocity with depth is consistent with the nature of limestone bedrock in the study area. More specifically, the uppermost limestone bedrock (<2 ft depth) is frequently described on MoDOT logs as highly weathered. The underlying limestone is typically described as gray, medium grained and medium hard. At many test sites multiple thin (<1 ft thick) clay layers were encountered within limestone bedrock. In general, the quality of limestone increased with depth from top of rock.

Depth to acoustic bedrock varies between 20 and 44 ft along the length of the MASW profile. Depths are believed to be accurate to within one-half of an MASW sample interval (accurate to within ~$\pm$2.5 ft). *Note: MASW depths to bedrock at all station locations were based on the interpretation of the smoothed acoustic bedrock horizon on Figure 7. Depths were not estimated from individual MASW curves.*

11. COMPARISON OF MASW AND BOREHOLE CONTROL

SCPT and bedrock (borehole) control was acquired at a number of locations in the study area (Figures 1a-d). All of the SCPT and most of the borehole (bedrock) locations were more than 50 ft from the MASW profile. For evaluation and comparative purposes, selected representative SCPT curves and borehole control is presented herein and "tied" to the nearest MASW station.

SCPT Site A6429-2 (Station 872+84.3, 26'RT, Elev. 477.1):

The SCPT A6429-2 shear-wave seismic velocity curve and the MASW station #1 shear-wave velocity curve are plotted in Figure 8. The elevation of the SCPT site A6429-2 (477.1 ft) is used as a reference datum (Figure 8). MASW station #1 elevation is 455 ft. Hence, the MASW station #1 curve "ties" the A6429-2 SCPT curve at a depth of approximately 22 ft. SCPT site A6429-2 is located off-line (re: 2-D MASW profile; Figures 1a-1d) and more than 50 ft from MASW station #1 (nearest MASW station).

Bedrock was not encountered by the SCPT tool, however moderately hard limestone was encountered in an adjacent borehole (A6429-2) at a depth of 50.8 ft (426.3 ft elevation). Bedrock at the SCPT A6429-2 site is therefore estimated to be at an elevation of 426.3 ft. Depth to acoustic bedrock at the

MASW station #1 location is estimated to be at an elevation of ~427 ft. (*Note: MASW acoustic bedrock is estimated to be at a sub-pavement depth of ~28 ft on MASW profile; Figure 7.*) The difference between the borehole depth-to-bedrock and the MASW depth-to-bedrock is only 0.7 ft.

The uppermost 28 ft (22-50 ft depth interval; Figure 8) of the subsurface at MASW station #1 location is characterized by MASW shear-wave velocities of between ~550 and ~1000 ft/s (Figure 8). This zone consists of pavement and compacted fill and soil. The corresponding depth interval at the SCPT site (as per available CPT data) is comprised predominantly of clayey silt to silty clay, sandy silt to clayey silt, and silty sand to sandy silt. It is characterized by SCPT shear-wave velocities ranging from ~700 ft/s to ~890 ft/s.

As shown on Figure 8, the MASW shear-wave velocities and the SCPT shear-wave velocities correlate reasonably well despite the physical separation between the two locations, the propensity for soil lithologies to vary laterally over short distances, and the fact that SCPT site is located on the embankment adjacent to interstate I-70 whereas the MASW site is on a paved section of interstate I-70.

The MASW shear-wave velocities at station #1 are believed to be reliable. This conclusion is based on the fact that the MASW depth to bedrock estimate correlates very well with available ground truth.

SCPT Site A6426-10 (Station 49+33.8, 15'RT, Elev. 475.8):

SCPT site A6426-10 is located off-line (re: 2-D MASW profile; Figures 1a-1d) and more than 50 ft from station #24 (nearest MASW station). SCPT site A6426-10 is at an elevation of 475.8 ft; MASW station #24 is at an elevation of 446 ft. The SCPT A6426-10 shear-wave seismic velocity curve and MASW station #24 are plotted in Figure 9. MASW trace #24 ties the SCPT curve at a depth of approximately 30 ft.

Bedrock was not encountered by the SCPT tool, however medium hard limestone was encountered in an adjacent borehole (A6426-10) at a depth of 52.1 ft (423.6 ft elevation). Bedrock at the A6426-10 SCPT site is therefore estimated to be at an elevation of 423.6 ft. Depth to acoustic bedrock at MASW station #24 is estimated to be at an elevation of 425 ft. (*Note: MASW acoustic bedrock is estimated to at a sub-pavement depth of 21 ft on MASW profile; Figure 7.*) The difference between the borehole depth-to-bedrock and the MASW depth-to-bedrock is only 1.4 ft.

The uppermost ~21 ft (30-51 ft depth interval) of the subsurface at MASW station #24 location is characterized by MASW shear-wave velocities of between ~500 and ~1000 ft/s (Figure 9). This zone consists of pavement and compacted fill and soil. The corresponding depth interval (as per MoDOT CPT data) at the SCPT site is comprised predominantly of silty clay to clay, clayey silt to silty clay, sandy silt to clayey silt, silty sand to sandy silt, and sand to silty sand. It is characterized by SCPT shear-wave velocities ranging from ~650 ft/s to ~910 ft/s (Figure 9).

As noted, the MASW shear-wave velocities and the SCPT shear-wave velocities correlate reasonably well despite the physical separation between the two locations, the propensity for soil lithologies to vary laterally over short distances, and the fact that SCPT site is located on the embankment adjacent to I-70 whereas the MASW site is on interstate I-70. The MASW shear-wave velocities are believed to be reliable because the estimated depth to acoustic bedrock at the MASW test site appears to be fairly accurate. {Note that the reliability of the SCPT curve is somewhat suspect because it has assigned an anomalously high shear-wave velocity of 1500 ft/s to a 3 ft interval comprised mostly of silty clay to clay (10-13 ft interval; Figure 9)}.

Borehole B-39 (Station 906+72.2, 81.9' LT):

In Figure 10, MASW station #84 is "tied" to borehole lithologic log B-39 (Figures 1a-1d). The B-39 borehole datum is at an elevation of 451.6 ft; the MASW datum is 453 ft.

The MASW station #84 shear-wave velocity curve correlates reasonably well with the B-39 borehole log. More specifically, the uppermost ~7 ft (comprised of pavement and compacted fill) is characterized by MASW shear-wave velocities of between ~650 and ~800 ft/s; lean clay is characterized by velocities between ~500 and ~750 ft/s; sandy silt is characterized by velocities of ~750 ft/s; limestone is characterized by velocities in excess of 1000 ft/s. The depths to limestone bedrock at the B-39 borehole and MASW locations (29.0 ft and 30.6 ft respectively; Figure 10) correlate well considering the test locations are separated by more than 50 ft. (*Note: MASW acoustic bedrock is estimated to at a sub-pavement depth of 32 ft on MASW profile; Figure 7.*) The difference between these two depths to bedrock is only 1.6 ft.

The MASW shear-wave velocities are believed to be reliable because the MASW estimated depth to acoustic bedrock appears to be fairly accurate.

SCPT Site A6433-10 (Station 3+78.5, 44.7'RT, Elev. 463.0):

SCPT site A6433-10 is located off-line (re: 2-D MASW profile; Figures 1a-1d) and more than 50 ft from station #87 (nearest MASW station). SCPT site A6433-10 is at an elevation of 463.0 ft; the MASW station #87 datum is at an elevation of 451 ft. The SCPT A6433-10 shear-wave seismic velocity curve and MASW station #87 are plotted in Figure 11. MASW station #87 ties the SCPT curve at a depth of approximately 12 ft.

Bedrock was not encountered by the SCPT tool, however a limestone layer was encountered at the A6433-10 borehole site at a depth of 54.2 ft (408.5 ft elevation). Bedrock at the SCPT A6433-10 site is therefore estimated to be at 408.5.0 ft elevation. Depth to acoustic bedrock at MASW station #87 is estimated to be at an elevation of 417 ft elevation. (*Note: MASW acoustic bedrock is estimated to at a sub-pavement depth of 34 ft on MASW profile; Figure 7.*) The difference between these two depths to bedrock is 8.5 ft.

The uppermost ~34 ft (12-46 ft depth interval) of the subsurface at MASW station #87 location is characterized by MASW shear-wave velocities of between ~500 and ~1000 ft/s (Figure 11). This zone is thought to consist primarily of pavement, compacted fill and soil. The corresponding depth interval at the SCPT site (as per MoDOT CPT data) is comprised predominantly of clay, silty clay to clay, clayey silt to silty clay, sandy silt to clayey silt, and silty sand to sandy silt. It is characterized by SCPT shear-wave velocities ranging from ~220 ft/s to ~800 ft/s. The average SCPT shear-wave velocity is approximately 540 ft/s (Figure 11).

As noted, the MASW shear-wave velocities and the SCPT shear-wave velocities correlate reasonably well despite the physical separation between the two locations, the propensity for soil lithologies to vary laterally over short distances, and the fact that SCPT site is located on the embankment adjacent to interstate I-70, whereas the MASW site is on I-70. The MASW shear-wave velocities are believed to be reliable even though the MASW estimated depth to acoustic bedrock and the borehole depth to bedrock differ by 8.5 ft. Our confidence, in part, is based on the fact that other A6433 boreholes encountered bedrock at elevations that are more consistent with the MASW estimate of 417 ft. For examples, borehole A6433-12 encountered bedrock at an elevation of 417.0 ft; borehole A6433-6 encountered bedrock at an elevation of 420.4 ft. These other two borehole depths to bedrock are consistent with the MASW depth of 417 ft.

{Note that the SCPT curve is somewhat suspect because it has assigned an unreasonably high shear-wave velocity of 4560 ft/s to a 3 ft interval comprised mostly of clay, silty sand, sandy silt and sand (3.5-6.5 ft interval; not shown in Figure 11)}.

SCPT Site A6440-10 (Station 3+12.8, 6.3'RT, Elev. 463.3):

SCPT site A6440-10 is located off-line (re: 2-D MASW profile; Figures 1a-1d) and more than 50 ft from station #110. SCPT site A6440-10 is at an elevation of 463.3 ft; MASW station #110 is at an elevation of 460 ft. The SCPT A6440-10 shear-wave seismic velocity curve and MASW station #110 are plotted in Figure 12. MASW station #110 ties the SCPT curve at a depth of approximately 3 ft.

High-velocity (~2170 ft/s) sand was encountered at a depth of 45.5 ft (elevation of 417.8 ft; Figure 12) at the SCPT test site. The top of these sands represent acoustic bedrock. Acoustic bedrock at MASW station #110 is estimated to be at an elevation of ~416 ft. (*Note: MASW acoustic bedrock is estimated to at a sub-pavement depth of 44 ft on MASW profile; Figure 7.*) The difference between these two depths to "acoustic" bedrock is ~1.8 ft.

The uppermost ~44 ft (3-47 ft depth interval) of the subsurface at MASW station #110 location is characterized by MASW shear-wave velocities of between ~600 and ~1000 ft/s (Figure 12). This zone consists primarily of pavement, compacted fill and soil. The corresponding depth interval at the SCPT site (as per MoDOT CPT data) is comprised predominantly of clay, silty clay to clay, clayey silt to silty clay, sandy silt to clayey silt, silty sand to sandy silt, and sand to silty sand. It is characterized by SCPT shear-wave velocities ranging from ~300 ft/s (not shown) to ~980 ft/s, and underlain by dense sand with an SCPT interval velocity of ~2500 ft/s (Figure 12).

As noted, the MASW and SCPT shear-wave velocities correlate reasonably well despite the physical separation between the two test locations, the propensity for soil lithologies to vary laterally over short distances, and the fact that SCPT site is located on an embankment adjacent to interstate I-70, whereas the MASW site is on I-70. However, the SCPT velocities are somewhat suspect because of the presence of an interval of unreasonably low (~-2280 ft/s) within a 3 ft interval (3-6 ft; not shown), and an interval of unreasonably high shear-wave velocities (~1400 ft/s) within a 6 ft interval (6-12 ft; Figure 12) comprised mostly of clay, silty clay and clayey silt.

The MASW shear-wave velocities are believed to be more reliable than the SCPT velocities because of the presence of the anomalous SCPT velocity values and because the estimated depth to acoustic bedrock at the MASW test site appears to be fairly accurate.

SCPT Site A6434-10 (Station 3+52.2, 27.1'LT, Elev. 453.4):

SCPT site A6434-10 is located off-line (re: 2-D MASW profile; Figures 1a-1d) and more than 50 ft from station #140 (nearest MASW station). SCPT site A6434-10 is at an elevation of 453.4 ft; the MASW station #140 datum is at an elevation of 440 ft. The SCPT A6434-10 shear-wave seismic velocity curve and MASW station #140 are plotted in Figure 13. MASW station #140 (0 ft depth) ties the SCPT curve at a depth of approximately 13 ft.

Hard limestone bedrock was not encountered at the SCPT site, however it was encountered at a proximal borehole site (A6434-7) at an elevation of 414.0 ft. Limestone bedrock at the SCPT A6440-10 site is therefore estimated to be at 414.0 ft elevation. Depth to acoustic bedrock at MASW station #140 is also estimated to be at an elevation of 414 ft. (*Note: MASW acoustic bedrock is estimated to at a sub-pavement depth of 26 ft on MASW profile; Figure 7.*)

The uppermost ~26 ft (13-39 ft depth interval) of the subsurface at MASW station #140 location is characterized by shear-wave velocities of ~450 ft/s to ~1000 ft/s (Figure 13). This zone consists primarily of pavement, compacted fill and soil. The corresponding depth interval at the SCPT site (as per MoDOT CPT data) is comprised predominantly of organic material, clay, silty clay to clay, clayey silt to silty clay, sandy silt to clayey silt, silty sand to sandy silt, and sand to silty sand. It is characterized by SCPT shear-wave velocities ranging from ~440 ft/s to ~900 ft/s (Figure 13).

As noted in Figure 13, the MASW and SCPT shear-wave velocities correlate fairly well despite the physical separation between the two test locations, the propensity for soil lithologies to vary laterally over short distances, and the fact that SCPT site is located on an embankment adjacent to interstate I-70 - whereas the MASW site is on I-70. The MASW shear-wave velocities are believed to be reliable because the estimated depth to acoustic bedrock at the MASW test site appears to be fairly accurate.

Borehole B-44 (Station 936+90.7, 82.6' RT):

In Figure 14, MASW station #159 is "tied" to borehole log B-44. The B-44 borehole datum is at an elevation of 447.8 ft; the MASW datum is 445 ft.

The MASW station #159 shear-wave velocity curve correlates well with the B-44 borehole log. More specifically, the uppermost 28 ft (3'-31' depth interval; Figure 14) is characterized by MASW shear-wave velocities of ~400 to ~1000 ft/s. The corresponding interval at the B-44 site is comprised of fill and lean clay. The B-44 borehole and MASW station # 159 depths to bedrock (29.5 ft and 30.8 ft respectively; Figure 14) correlate very well considering the test sites are separated by more than 50 ft. (*Note: MASW acoustic bedrock is estimated to at a sub-pavement depth of 28 ft on MASW profile; Figure 7.*)

Suite of Seventeen Borehole Locations Presented in Table 1:

Seventeen boreholes are listed in Column B Table 1. Corresponding highway structures (Column A), borehole station locations (Column C), offsets (Column D), borehole elevations (Column E), borehole depths to bedrock (Column F) and borehole bedrock elevations (Column G) are tabled. Presented as well in Table 1 are the closest MASW station locations (Column H), and corresponding MASW datum elevations (Column I), estimated MASW depths to bedrock relative to MASW datum (Column J), and estimated MASW bedrock elevations (Column K). Depths in columns G and K can be compared directly.

The comparison of the borehole depths to bedrock (Column F) and the corresponding MASW estimated depths to acoustic bedrock (Column J), indicates that the MASW interpretations compare favorably to ground truth except in proximity to borehole A6440-13. Dense sand was encountered at an elevation of 415.3 ft (ASL) in the A6440-13 borehole. The top of this dense sand is thought to represent acoustic bedrock (as per discussion of SCPT Site A6440-10; Section 11 of Report).

On average (including depth differential to acoustic bedrock at borehole A6440-13 and MASW station 110), MASW estimated depths to bedrock exceed borehole depths to bedrock (as per Figure 17) by ~0.7 ft. This average depth differential is remarkably small, given the variable depth to bedrock in the study area and the fact that the boreholes were not situated exactly on the centerline of the MASW traverse.

12. CONCLUSIONS AND RECOMMENDATIONS

On the basis of the comparison of MASW-estimated bedrock depths and proximal ground truth (borehole control), it is concluded that the interpretation of the 2-D MASW shear-wave velocity profile is reasonably reliable (Figure 7). The implication is that the MASW shear-wave velocities are also reliable. Indeed, if this were not the case, the MASW horizons (as interpreted; Figure 7) would not correlate well (depth-wise) with available borehole control. It is recognized that all currently available borehole control is "off-line" and that comparative analyses are based on extrapolated "ties".

The acquisition of additional 2-D MASW data at select sites in Missouri is recommended, in an effort to assess the utility of this tool for locating karstic cavities within soil and/or bedrock.

13. SUGGESTED REFERENCES

Aki, K., and Richards, P.G., 1980, Quantitative Seismology: W.H. Freeman & Co., San Francisco, 932 p.

Bullen, K.E., 1963, An Introduction to the Theory of Seismology: Cambridge University Press, 381 p.

Herrmann, R.B., 1996, Computer Programs in Seismology: Saint Louis University Press, Saint Louis, Missouri.

Liu, H.P., Boore, D.M., Joyner, W.B., Oppenheimer, D.H., Warrick, R.E., Zhang, W., Hamilton, J.C., and Brown, L.T., 2000, Comparison of phase velocities from array measurements of Rayleigh waves associated with micro-tremor and results calculated from borehole shear-wave velocity profiles: Bulletin Seismological Society of America, **90**, 666-678.

Kramer, S.L., 1996, Geotechnical Earthquake Engineering: Prentice-Hall Inc., 653 p.

Miller, R.D., Xia, J., Park, C.B., and Ivanov, J., 2000, Shear-wave velocity field from surface waves to detect anomalies in the subsurface: Geophysics 2000, FHWA and MoDOT Special Publication, 4:8.1–4:8.10.

Nazarian, S., Stokoe, K.H., and Hudson, W.R., 1983, Use of spectral analysis of surface waves method for determination of moduli and thicknesses of pavement systems: Transportation Research Record, **930**, 38-45.

Park, C.B., Miller, R.D., and Xia, J., 1999, Multichannel analysis of surface waves: Geophysics, **64**, 800-808.

Park C.B., Miller, R.D., and Xia J., 1999, Multimodal analysis of high frequency surface waves: Proceeding of the Symposium on the Application of Geophysics to Engineering and Environmental Problems, 115-121.

Park, C.B., Miller, R.D., Xia, J., and Ivanov, J., 2000, Multichannel seismic surface-wave methods for geotechnical applications: Geophysics 2000, FHWA and MoDOT Special Publication, 4:7.1-4:7.11.

Press W.H., Teukolsky, S.A., Vetterling, W.T., and Flannery, B.P., 1997, Numerical Recipes in C: The Art of Scientific Computing: Cambridge University Press, 965 p.

Rechtien, D., 2002, Inversion of Liquefaction Relevant Seismic Data: U.S. Army Corps of Engineers Contract Report GL-02-1, 64 p.

Stokoe, K.H., Wright, G.W., James, A.B., and Jose, M.R., 1994, Characterization of geotechnical sites by SASW method, *in* Geophysical Characterization of Sites ISSMFE Technical Committee #10, edited by R.D. Woods: Oxford Publishers, New Delhi

Xia, J., Miller, R.D., and Park, C.B., 1999, Estimation of near-surface velocity by inversion of Rayleigh waves: Geophysics, **64**, 691-700.

Zywicki, D.J., and Rix, G.J., 1999, Frequency-wavenumber analysis of passive surface waves: Proceeding of the Symposium on the Application of Geophysics to Engineering and Environmental Problems, 75-84.

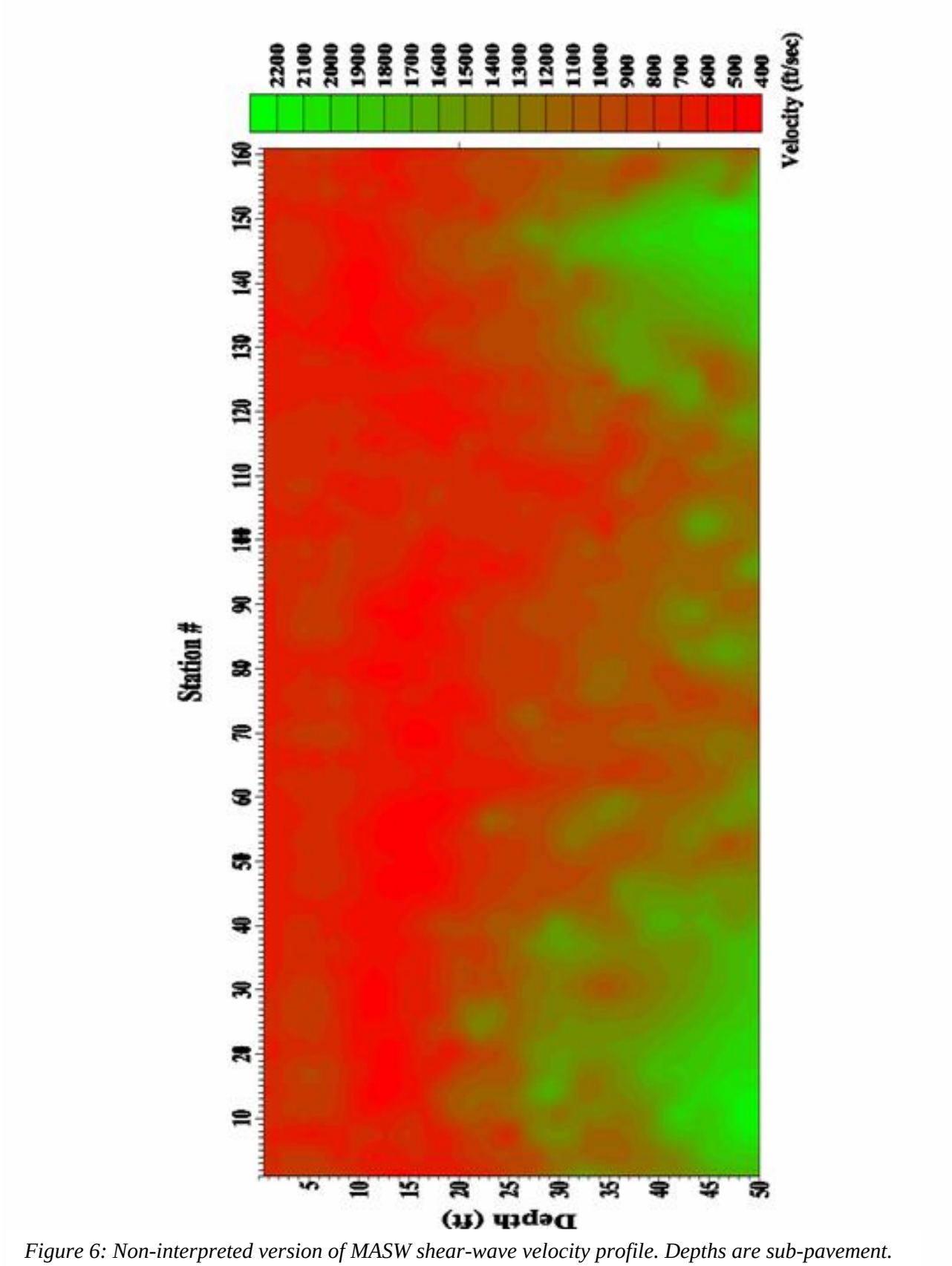

Figure 6: Non-interpreted version of MASW shear-wave velocity profile. Depths are sub-pavement.

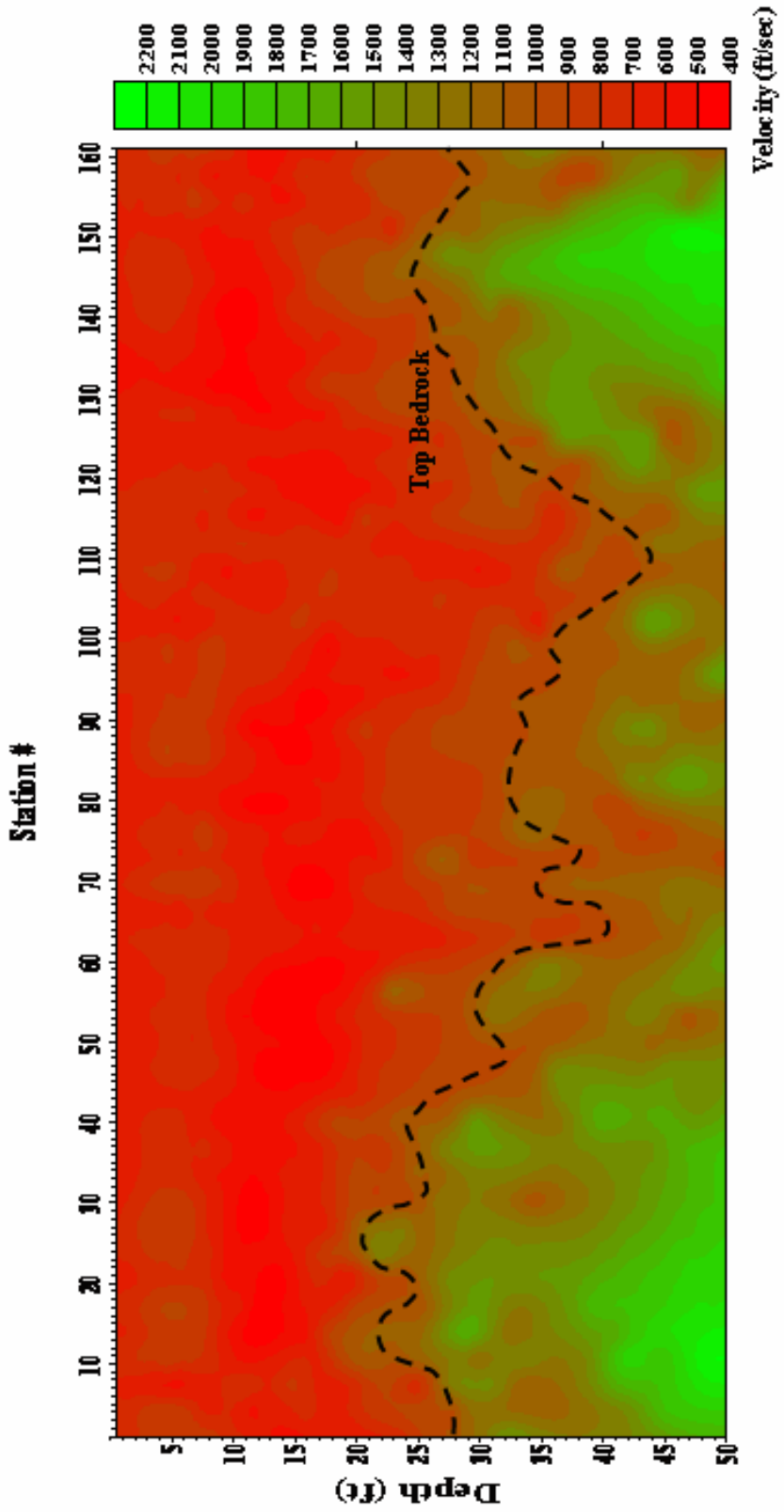

Figure 7: Interpreted version of MASW shear-wave velocity profile. Depths are sub-pavement.

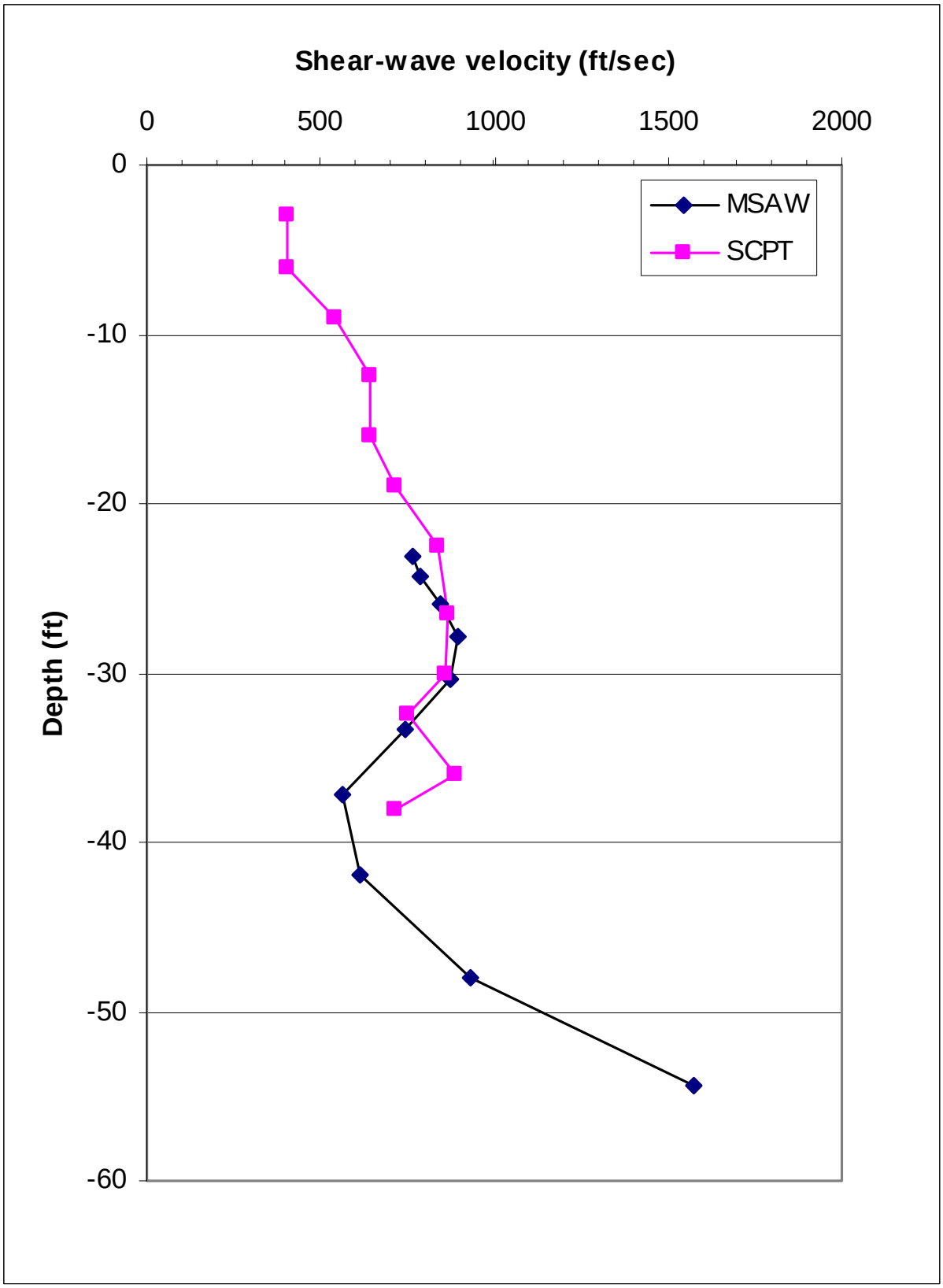

Figure 8: SCPT curve for site A6429-2 and MASW station #1. Datum elevation is 477.1 ft.

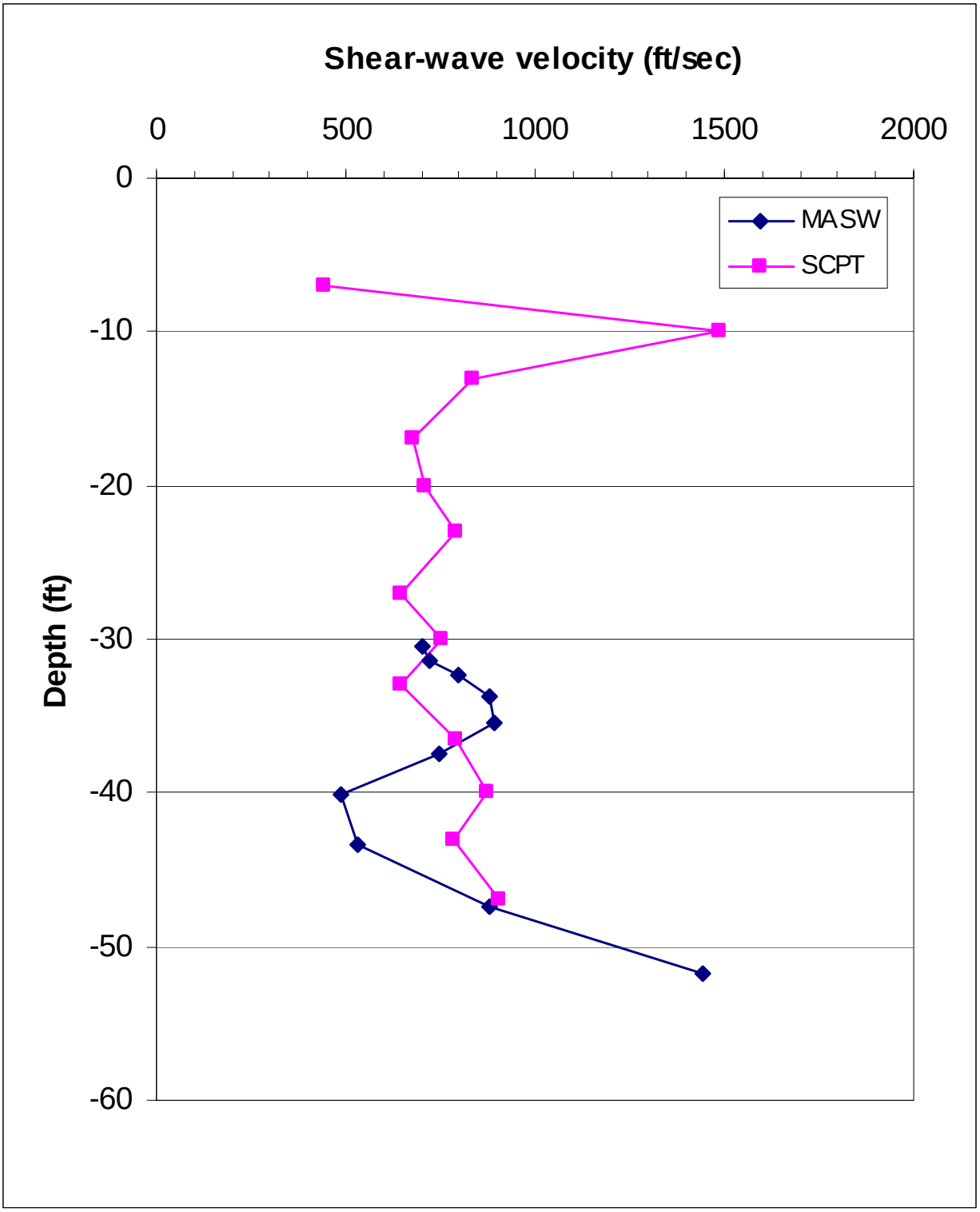

Figure 9: SCPT curve for site A6426-10 and MASW station #24. Datum elevation is 475.8 ft.

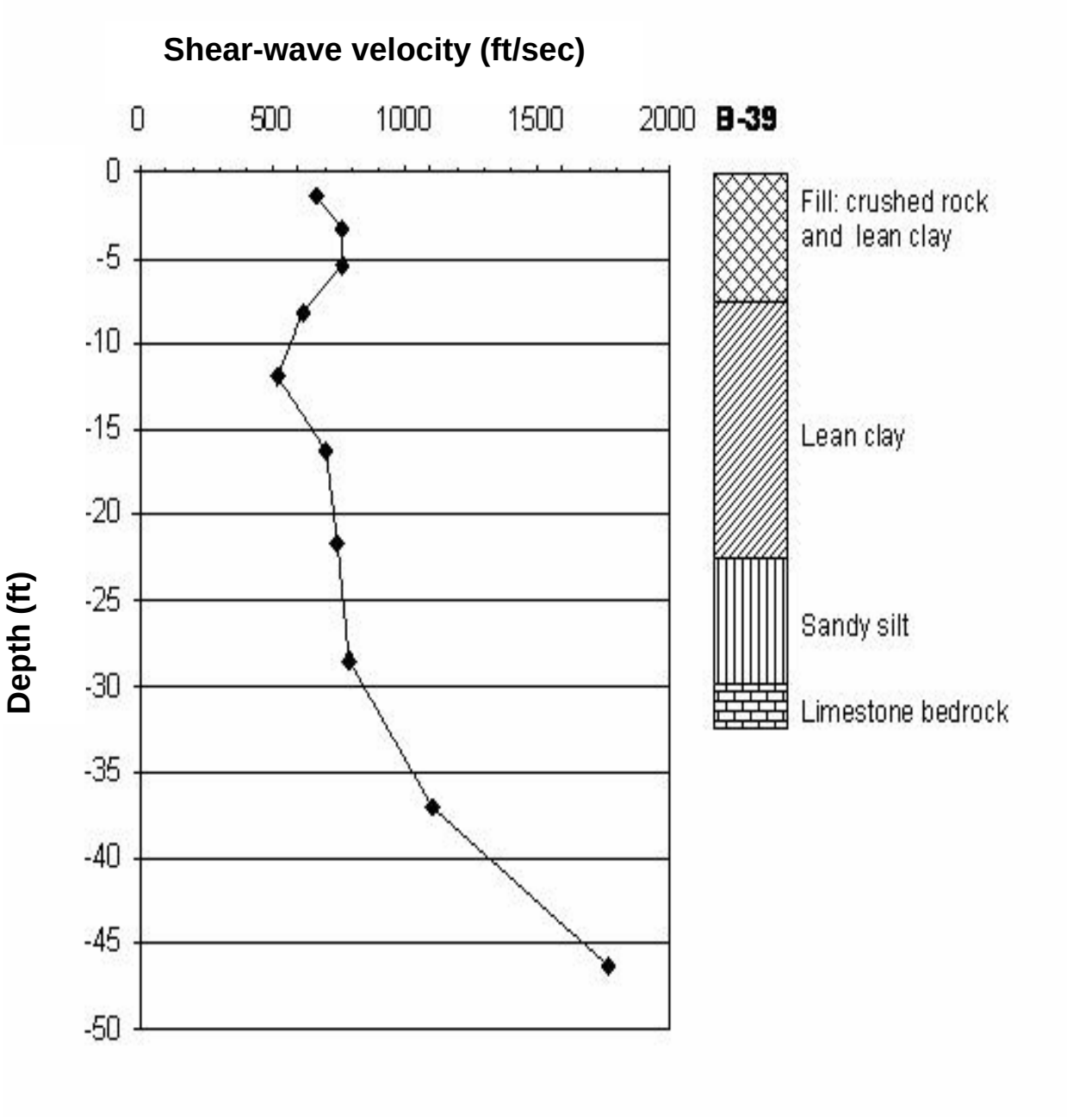

Figure 10: B-39 borehole lithologic log and MASW station #84.
Geologic log was provided by MoDOT. Datum elevation is 451.6 ft.

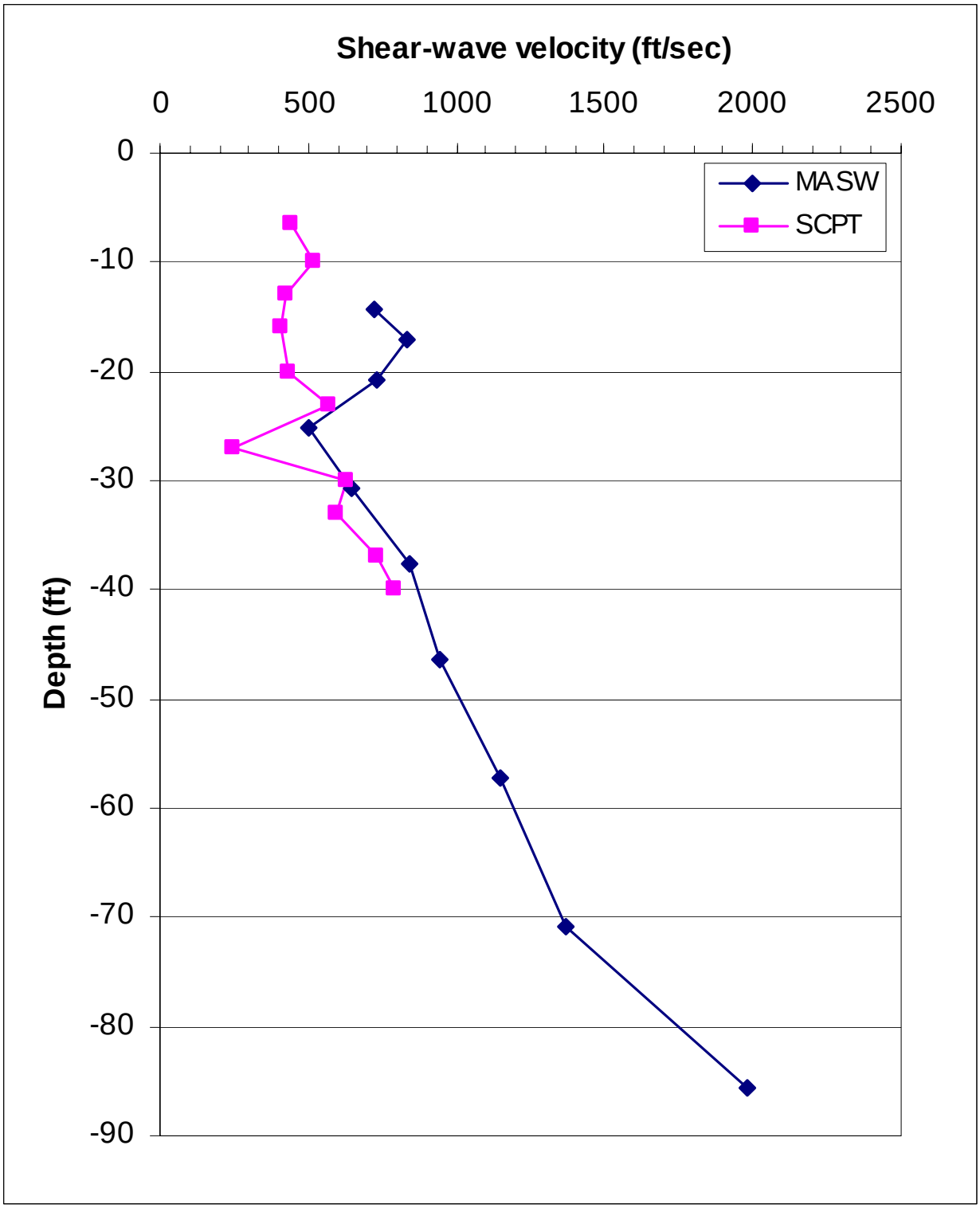

Figure 11: SCPT curve for site A6433-10 and MASW station #87. Datum elevation is 463.0 ft.

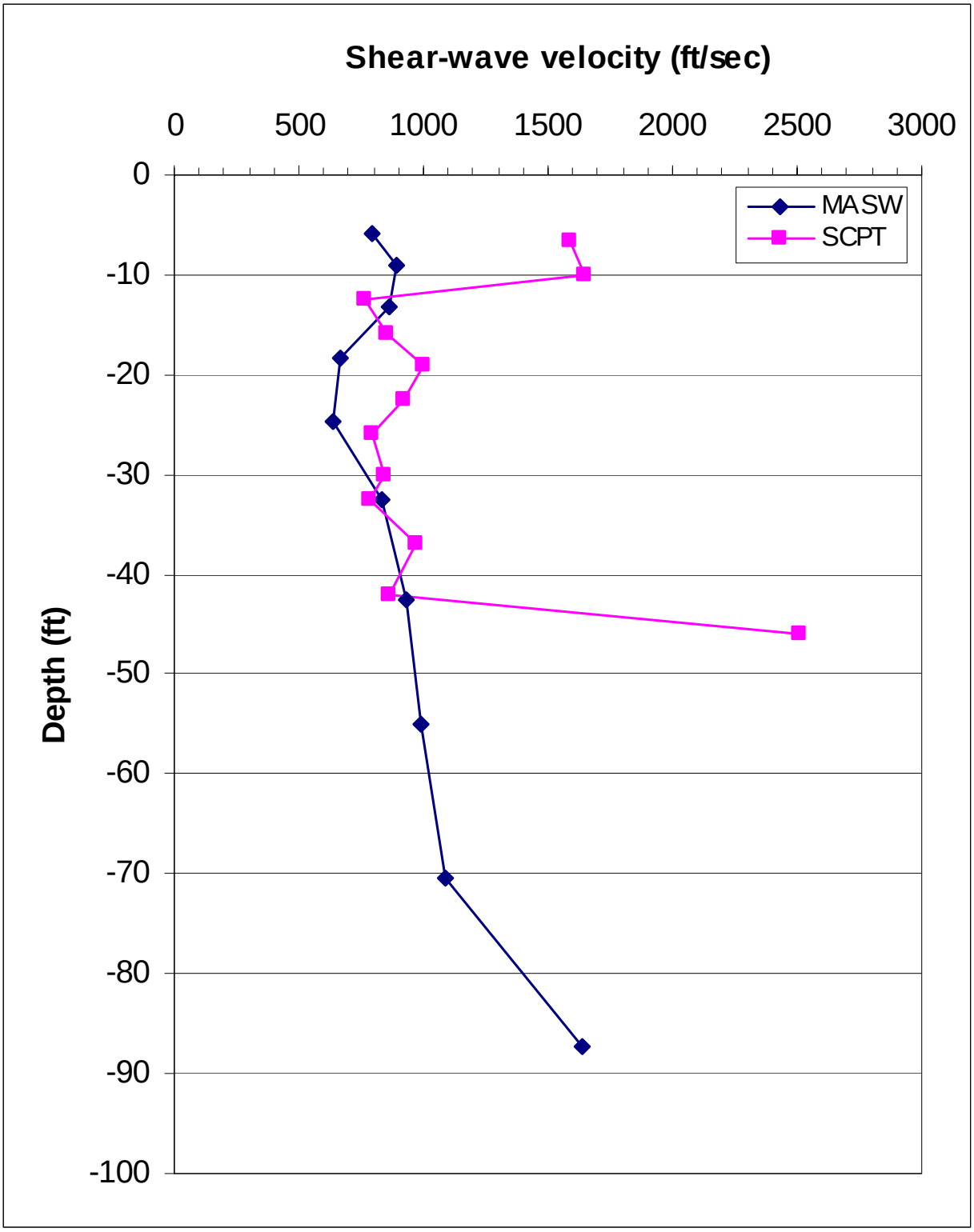

Figure 12: SCPT curve for site A6440-10 and MASW station #110. Datum elevation is 463.3 ft.

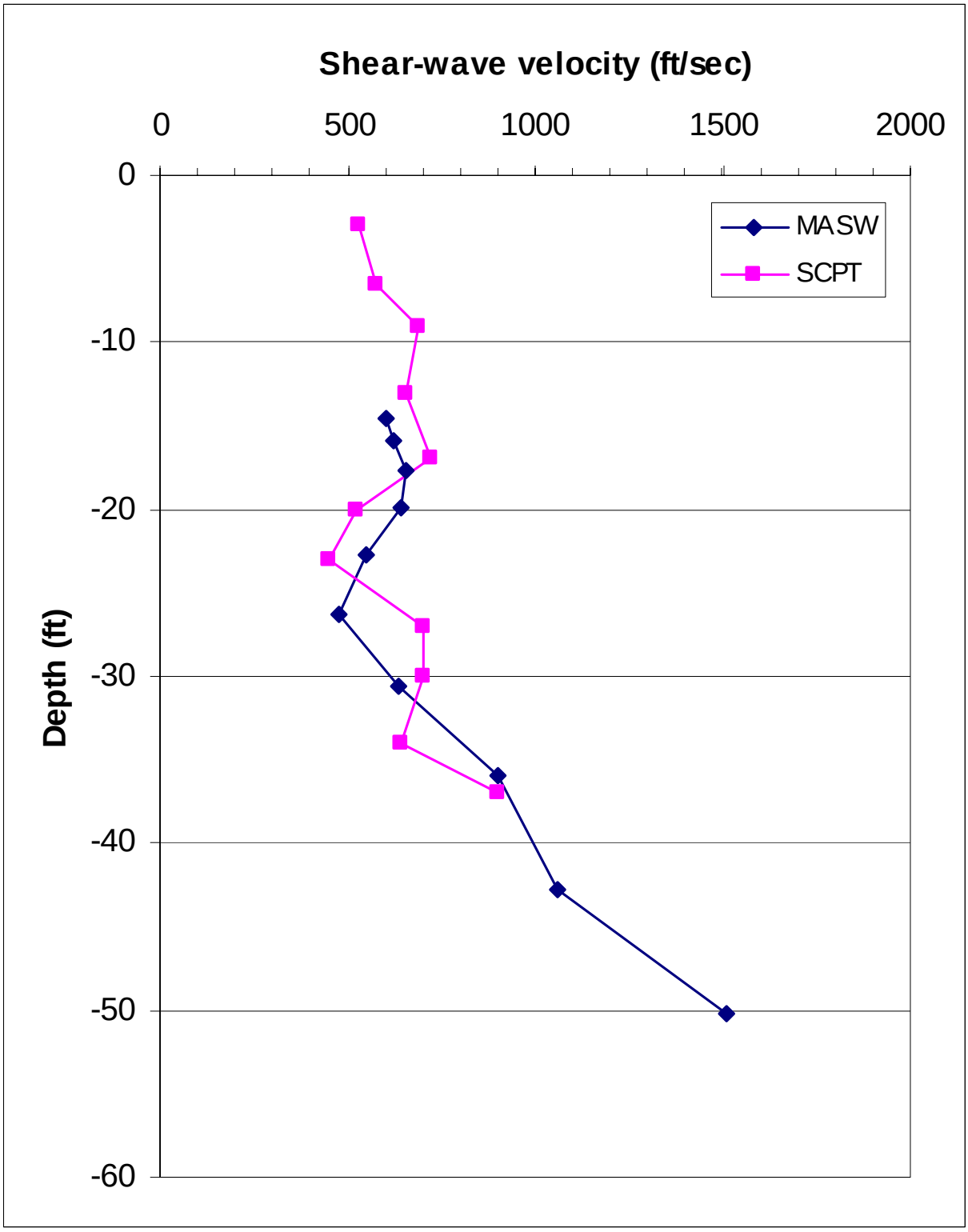

Figure 13: SCPT curve for site A6434-10 and MASW station #140. Datum elevation is 453.4 ft.

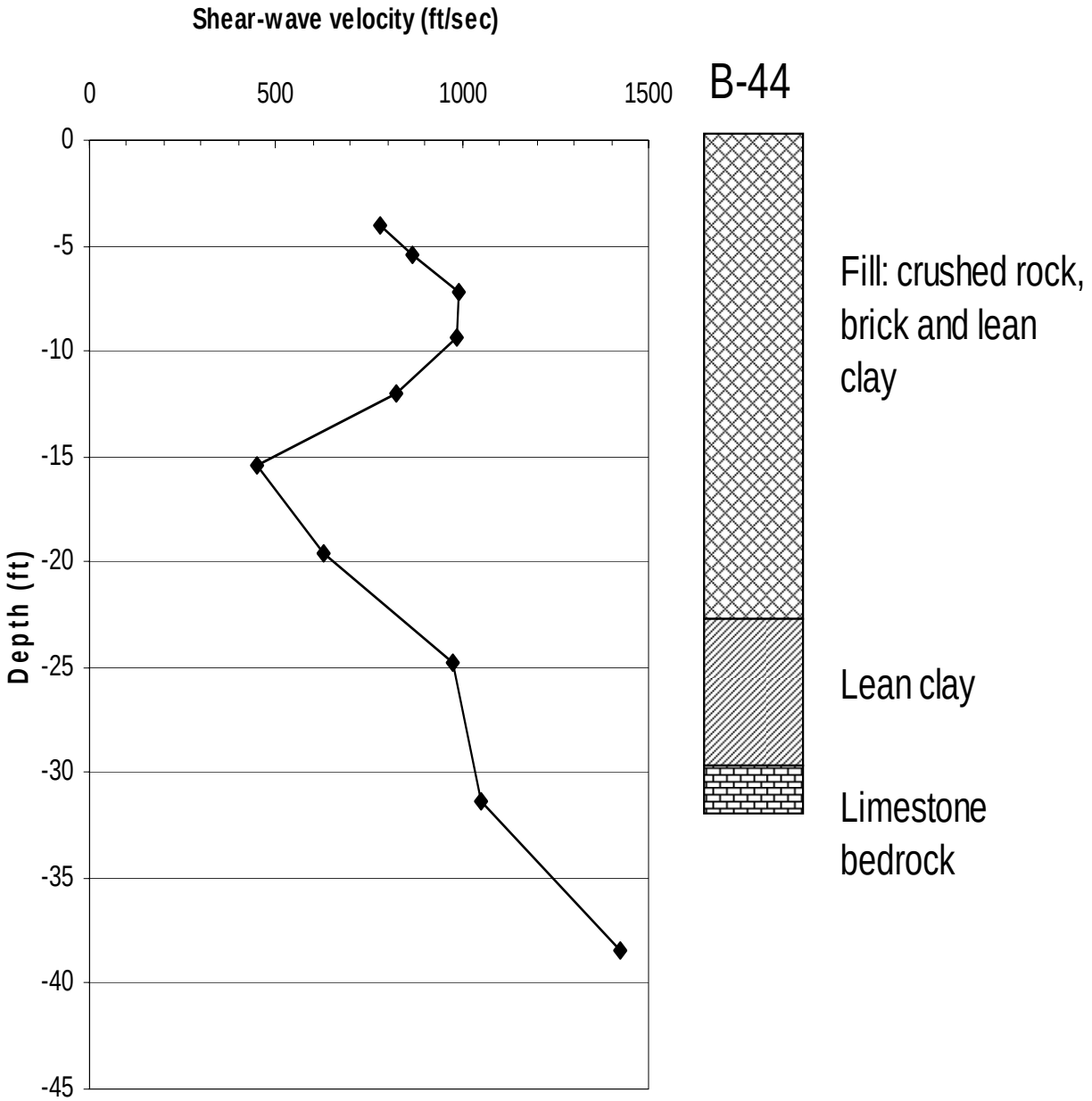

Figure 14: B-44 borehole lithologic log and MASW station #159. Geologic log was provided by MoDOT. Datum elevation is 447.8 ft.

Highway Structure (Fig. 1)	Highway Structure Borehole Number (BH#)	Highway Station of BH	Offset of BH (ft)	BH Elev. (ft)	BH Depth to Bedrock (ft)	BH Bedrock Elevation (ft ASL)	MASW Station (Fig. 7)	Elevation of MASW Station (ft)	MASW Depth To Bedrock (ft)	MASW Depth To Bedrock (ft ASL)
A	B	C	D	E	F	G	H	I	J	K
A6427	A6427-4	6+66.3	54' LT	448.9	19.2	429.7	11	451	22	429
A6426	A6426-5	47+13.1	6' LT	445.6	21.7	423.9	22	447	22	425
	A6426-6	47+16.82	15' RT	445.5	22.5	423.0	21	447	23	424
A6422	A6422-5	31+60.6	16.6' LT	448.6	20.3	428.3	41	448	23	425
A6525	A6525-8	10+47.3	1.7' RT	448.3	23.0	425.3	42	448	24	424
A6423	A6423-7	357+21.3	21' LT	447.8	19.5	428.3	41	448	23	425
A6424	A6424-13	456+08	0.5' RT	449.3	24.1	425.2	45	448	25	423
A6433	A6433-4	2+03.8	26' LT	448.0	25.7	422.3	86	452	32	420
	A6433-5	2+03.8	C/L	447.6	25.6	422.0	87	451	33	418
A6430	A6430-9	293+94	30' LT	459.5	37.8	421.7	68	459	35	424
A6440	A6440-13	5+31.5	C/L	459.8	44.5 DS#	415.3	109	460	44	416
					52.6 BR*	407.2				
A6434	A6434-1	2+07.8	33.6' LT	436.5	26.3	410.2	141	439	26	413
	A6434-2	2+02.7	C/L	435.6	21.6	414.0	140	440	26	414
	A6434-3	2+00.9	26' RT	435.9	20.4	415.5	139	441	26	415
	A6434-4	2+28.5	C/L	436.6	22.4	414.2	141	439	25	414
	A6434-5	2+27.4	C/L	435.8	21.3	414.5	140	440	26	414
	A6434-6	2+25.7	51.7' RT	436.2	23.2	413.0	138	441	27	414

Table 1: A comparison of borehole depths to bedrock at seventeen additional borehole locations and corresponding estimated MASW depths to bedrock (denotes depth to limestone bedrock; # denotes depth to dense sand).*